A 1×16 SiPM Array for Automotive 3D Imaging LiDAR Systems

Salvatore Gnecchi*, Carl Jackson*
*SensL Technologies, 6800, Cork Ariport Business Park, Cork, Ireland
{sgnecchi,cjackson}@sensl.com

***Abstract*—We present a vertical line sensor composed of a 1×16 array of analog silicon photomultipliers (SiPM) optimized for 3D time of flight (ToF) imaging LiDAR in advanced driver assistance systems (ADAS) and autonomous driving (AD) vehicles. The sensor has been designed for enhanced red-sensitivity performance with a PDE of greater than 8% and can operate in outdoor environments with high ambient light noise of $100\,\mathrm{klux}$ and targets that have a low reflectivity from 10%. The SiPM array enables long distance ranging greater than $100\,\mathrm{m}$ and allows for superior low reflective target distance ranging over APD and PIN diode based systems. The SiPM array is to be demonstrated in an electro-mechanical scanning imaging LiDAR system consisting of a transmitter based on an eye-safe $905\,\mathrm{nm}$ laser diode array the 1×16 SiPM array as receiver, collimating optics and an electro-mechanical rotating mirror for horizontal scanning of a $80° \times 5°$ at 30 fps. Simulation results are presented here to validate the concept of long distance LiDAR based on SiPM receivers.**

***Index Terms*—SiPM, Silicon Photomultipliers, Single Photon Avalanche Diodes, SPAD, LiDAR, ADAS, AD, 3D ToF.**

I. Introduction

Silicon Photomultipiers (SiPM) have been gaining increasing popularity over linear APDs in long distance LiDAR applications [1], [2], [3], such as advanced driver assistance systems (ADAS) and autonomous driving (AD) vehicles, due to their single-photon detection capability, uniformity when integrated into large arrays and low system cost. SiPM sensors are based on arrays of single photon avalanche photodiodes (SPAD) which are characterized by a high internal gain of $\sim 10^6$ when biased above their breakdown voltage in Geiger-mode. A single photon causes a macro-current to be generated at the output terminals which for SensL SiPM consists of three terminals: anode, cathode and fast output [4].

The single photon sensitivity of SPAD sensors is desired for low light applications such as long distance automotive LiDAR where the intensity of the return laser pulse is extremely weak due to the low reflectivity of the targets and the attenuation of the return laser power over the distance which varies as $1/\mathrm{distance}^2$. The high internal gain of SiPM sensors overcomes the low noise limitation of the amplification stage in linear avalanche photodiode (APD) and PIN diode sensors. The SPAD cell dead time τ_{dead}, due to quenching and recharging process, typically on the order of tens of nanoseconds, sets an upper limit to the maximum detected photon rate per SPAD equal to $1/(e \cdot \tau_{dead})$ [5].

The number of SPAD cells N_{cells} contribute to extend the dynamic range since the light can be spread over multiple SPAD sensors in each pixel reducing the average amount of photons incident on each SPAD by a factor equal to the number of cells [6], [7]. This is necessary for a large angle of view 3D ToF scanning system to avoid sensor saturation. The extended dynamic range can be written as:

$$\mathrm{DR}_{SiPM} = \frac{N_{cells}/(e \cdot \tau_{dead})}{\sqrt{\mathrm{DCR} + m_{amb}}} \tag{1}$$

where DCR is the dark count rate of the entire SiPM and m_{amb} is the average count rate due to uncorrelated ambient noise incident on the sensor. The process used to fabricate the SPAD sensors has been designed to enable a higher photo detection efficiency and a value of 8.4% has been obtained to date for this work. This high PDE is required to provide the long range detection probability planned for this work.

In this paper we discuss the challenge of SiPM based scanning LiDAR receivers and propose a 1×16 array of SiPM pixels optimized for outdoor LiDAR performing in a $100\,\mathrm{klux}$ environment and able to range low reflective objects at long range. Section II describes in detail the architecture of the pixel, the configuration in the chosen array and provides information on system level of the final 3D ToF scanning demonstrator. Section III presents the analysis on the predicted performance of the proposed array and Section IV offers conclusions and outlook of the presented work.

II. System and Pixel Architecture

A co-axial scanning LiDAR system consists of a laser beam scanning the scene in front of the sensor. A single set of optics are used to simplify alignment. The scan can be in both vertical and horizontal directions (a 2D scanning approach), in the case of a single point sensor; or in horizontal direction (a 1D scanning system), in the case of a vertical laser beam. Alternatively the scene can be illuminated with the laser light all together in a flash operation mode. While flash is appealing since no moving parts are necessary, the authors feel the requirements on laser power are still too restrictive to make it a reasonable option for long range, wide angle of view, automotive LiDAR. Alternatively, 2D scanning solutions offer the highest signal-to-noise case but they are mechanically too demanding in terms of rotating speed in order to operate at the desired

frame rates. For such reasons, a horizontal scanning system represents a useful trade-off and was developed in this work.

Shown in Fig. 1, the system is designed to use a vertical laser beam and an electro-mechanical rotating mirror to scan an $80° \times 5°$ scene. The electro-mechanical system can be changed to a MEMS mirror for a solid-state system. The horizontal divergence of the laser is set to $< 0.1°$ matching the angle of view of the sensor and therefore defining the horizontal angular resolution of the system. For the vertical axis, the resolution is given by the total angle of view divided by the number of pixels as $5°/16 = 0.312°$. A larger array or a different optical solution or both could be used to increase the total angle of view in the vertical direction if desired in future versions of the system. The speed of the scanning mirror is tunable and allows a frame rate of $30\,\mathrm{fps}$ to be achieved. The eye-safe laser provides a maximum total laser peak power of $400\,\mathrm{W}$. The incident light is collected through an aperture lens of diameter $D_{lens} = 22\,\mathrm{mm}$ to focus the light onto the sensor. The focal length is chosen to give the SiPM array the angle of view of $0.1° \times 5°$ required by the system using a simple optics setup. To improve the ambient light rejection, a bandpass filter is inserted in the optical path of the received light. The filter is centred around the laser wavelength and has a bandpass of $\pm 25\,\mathrm{nm}$. This level of bandpass filter is required in a system using 905 nm laser diodes which have a temperature dependent wavelength response on the order of $0.28\mathrm{nm}/°\mathrm{C}$. The SiPM pixel array has been designed to meet the requirements of dynamic range in extreme ambient light conditions maintaining a compact size. 133 SPAD cells of $20\,\mu\mathrm{m} \times 20\,\mu\mathrm{m}$ active area have been arranged in a $171\,\mu\mathrm{m} \times 491\,\mu\mathrm{m}$ pixel. Each pixel is spaced by $59\,\mu\mathrm{m}$ from its next neighbour to minimize optical cross-talk among adjacent pixels. The photo detection efficiency (PDE) of the sensor is targeted to reach $8.4\,\%$ at the chosen wavelength of $905\,\mathrm{nm}$. Each fast output of the analogue SiPM pixels is amplified by a TIA and then connected to a programmable comparator whose output feeds a time-to-digital converter on FPGA for the time-of-flight measurement.

The performance of the system is analyzed in the next Section while all the system parameters are summarized in Table I.

III. Modeled Performance of Scanning System

The performance of the sensor in the described scanning LiDAR system is analyzed in terms of signal, noise and probability of detection of the return laser pulse. We start the analysis with the calculation of the noise level.

a) Noise floor calculation: The noise floor at the pixel level ($N_{pixels} = 16$) is determined by the amount of ambient light incident on the sensor. Assuming a worst case of full $100\,\mathrm{klux}$ sunlight illuminating the target, the optical power at the aperture, focused on the sensor is calculated as:

$$P_{amb} = \mathfrak{P}_{amb} \cdot A_{FoV} \cdot \frac{1}{2\pi d^2} \cdot \eta \cdot A_{aperture} \cdot \frac{1}{N_{pixels}} \quad (2)$$

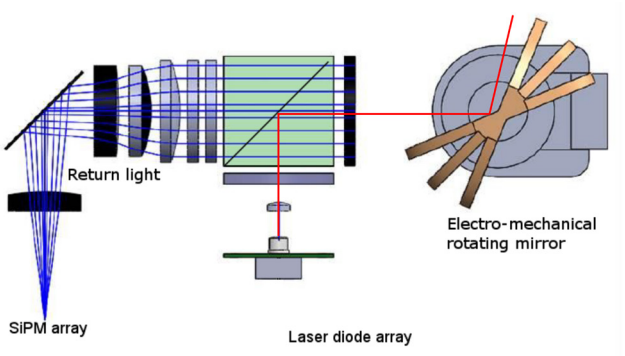

Figure 1. **Coaxial 1D Scanning System** - A vertical laser beam is scanned horizontally with the usage of an electromechanical mirror which also focuses the return light back onto a 1×16 SiPM array. A polarizer beam splitter is used to direct the transmitted light onto the rotating mirror. The return light sees a worst-case reduction in intensity of 50%.

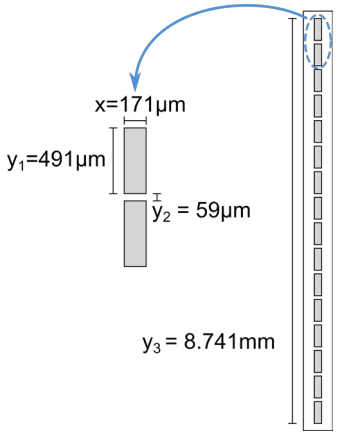

Figure 2. **SensL 1×16 SiPM Array** - The sensor consists of a monolithic array of 16 pixels in a vertical line. The dimensions are reported in Table I. The geometry of the pixels follows the required angle of view in both horizontal and vertical direction.

The term $\mathfrak{P}_{amb}$ represent the solar power density contributing to the noise level; it depends on the chosen bandpass filter and can be calculated from the solar spectral irradiance[8] $\mathfrak{I}_{sun}$ as

$$\mathfrak{P}_{amb} = \int_{\lambda-\Delta\lambda}^{\lambda+\Delta\lambda} \mathfrak{I}_{sun}(\lambda')d\lambda' \quad (3)$$

A_{FoV} represents instead the area of the field of view at the distance d and it is calculated as

$$A_{FoV} = 4d^2 \cdot \tan\left(\frac{AoV_x}{2}\right) \cdot \tan\left(\frac{AoV_y}{2}\right) \quad (4)$$

The product of the first two terms in (2) represents the incident power on the field of view. This is then diffused back onto the sensor by target in the field of view (here assumed to cover the entire area). The diffusive nature of the target is modeled by a reflectivity parameter η (between 0 and 1). Moreover, the intensity of the returned diffused light is modeled to decrease with the square of the distance as expressed by the term $1/(2\pi d^2)$ in (2). The power density

Table I
SENSL LIDAR SYSTEM PARAMETERS

Parameter	Value
Array size	1×16
SiPM pixel length x	171 µm
SiPM pixel height y_1	491 µm
Pixel spacing y_2	59 µm
Total array length y_3	8.741 mm
SPAD cells per pixel N_{cells}	133
PDE @ 905 nm	8.4 %
SPAD cell dead time τ_{dead}	23ns
SiPM pixel gain G	10^6
SiPM rise time τ_{rise}	100 ps
Laser divergence	$0.1° \times 5°$
Laser peak power P_{laser}	400 W
Laser pulse width τ_{pulse}	1 ns
Laser pulse repetition rate PRR	500 kHz
Frames per second	30 fps
Optical aperture D_{lens}	22 mm
Scanning angle of view	$80° \times 5°$
Static angle of view $AoV_x \times AoV_y$	$< 0.1° \times 5°$
Angular resolution	$0.1° \times 0.312°$
Optical bandpass $\lambda \pm \Delta\lambda$	(905 ± 25) nm

at the distance d, where the aperture is placed, is collected by the receiving lens whose area is expressed by

$$A_{aperture} = \pi \frac{D_{lens}^2}{4} \tag{5}$$

To convert the incident optical power per pixel into a photon rate, we divide the power by the average energy of the single photon $\Phi_{amb} = P_{amb}/(hc/\lambda)$. The detected noise floor can be expressed in terms of average number of cells per pixel fired due to continuous sunlight:

$$N_{amb} = N_{cells} \cdot \left(1 - e^{-\Phi_{amb} \cdot PDE \cdot \tau_{dead}/N_{cells}}\right) \tag{6}$$

Note that the ambient light level does not depend on the target distance since the two terms of d^2 cancel each other out of (2). It however depends on system parameters such as the angle of view of the pixel, the central wavelength and the filter bandpass.

b) Signal level calculation: The intensity of the return laser pulse per pixel can be calculated similarly to (2) assuming that all the incident laser power onto the target is diffused back onto the aperture:

$$P_{return}(d) = P_{laser} \cdot \frac{1}{2\pi d^2} \cdot \eta \cdot A_{aperture} \cdot \frac{1}{N_{pixels}} \tag{7}$$

from which the average return photon rate is $\Phi_{return} = P_{return}/(hc/\lambda)$. The detected signal can be now calculated as the average number of cells within the pixel N_{laser} firing due to laser photons. However, since the SiPM pixel is not a linear system, the signal level cannot be calculated independently from the noise level: due to the dead time, the detection of noise might inhibit the detection of laser photons. N_{laser} is calculated as

$$N_{laser}(d) = (N_{cells} - N_{amb}) \times \left(1 - e^{-\Phi_{return} \cdot PDE \cdot \tau_{pulse}/N_{cells}}\right) \tag{8}$$

c) Laser detection probability: The probability of detecting the return laser pulse is here analyzed considering the described threshold system. The noise floor of the SiPM, proportional to the square root N_{amb}, is used to set the threshold of the comparator. Let us assume a convenient level th equal to $2.5 \cdot \sqrt{N_{amb}}$. The probability of detecting the return laser is therefore equal to the probability of the signal to exceed such value. Assuming a Gaussian distribution around N_{laser} and a standard deviation $\sigma_s = \sqrt{N_{amb} + N_{laser}}$, the probability of having a signal higher than the threshold th is:

$$p_{signal}(d) = \frac{1}{\sqrt{2\pi\sigma_s}} \int_{th}^{\infty} \exp - \frac{(N - N_{laser}(d))^2}{2\sigma_s^2} dN \tag{9}$$

However, exceeding the threshold with the signal level is not sufficient for a successful measurement. In fact, the threshold can be exceeded also by the noise itself with a probability of:

$$p_{noise} = \frac{1}{\sqrt{2\pi\sigma_n}} \int_{th}^{\infty} \exp - \frac{N^2}{2\sigma_n^2} dN \tag{10}$$

where $\sigma_n = \sqrt{N_{amb}}$ is the standard deviation of the noise level. Often, p_{noise} is referred to as *probability of false alarm*. This can be minimized by increasing the threshold although the detection of the signal is also reduced. From (9) and (10), the probability of a successful measurement can be estimated by

$$p_{success}(d) = p_{signal}(d) - p_{noise} \tag{11}$$

d) Multi-shot approach: To improve the performance and increase the probability of measurement, a *multi-shot* approach can be adopted. LiDAR systems needs to operate at a certain frame rate which, together with the size of the frame itself, sets the maximum amount of time for a measurement to occur before the next point or frame are measured. For a 1D horizontal scanner such as the one proposed by this work, the frame size consists of the number of steps needed to cover the entire scene $80°/0.1° = 800$, since the vertical axis is measured in parallel by the 16 pixels. The maximum amount of time for a measure to be acquired is therefore given by

$$T_{meas} = \frac{1}{\text{FPS} \cdot 800} = 41\,\mu\text{s} \tag{12}$$

With a sufficient high laser pulse repetition rate PRR, more than a single measurement can be obtained in this amount of time:

$$\mathcal{N}_{pulse} = T_{meas} \times \text{PRR} = 20 \tag{13}$$

Acquiring $\mathcal{N}_{pulse}$ pulses per measurements allows the probability of a successful measurement to be improved. In fact, for each set of $\mathcal{N}_{pulse}$ single-shot measurements, an average

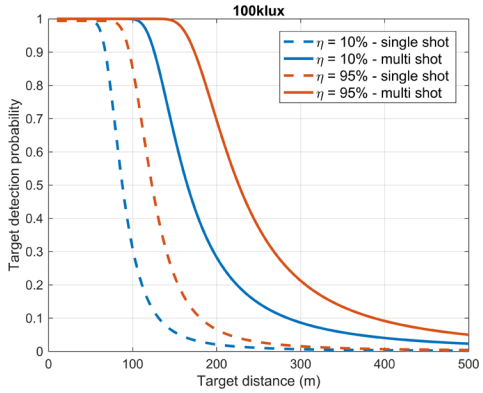

Figure 3. **Array performance at 100 klux** - The probability of detecting the return laser depends on the distance and the reflectivity of the target within the field of view. No sensor saturation occurs. The multishot approach allows longer distances to be efficiently ranged.

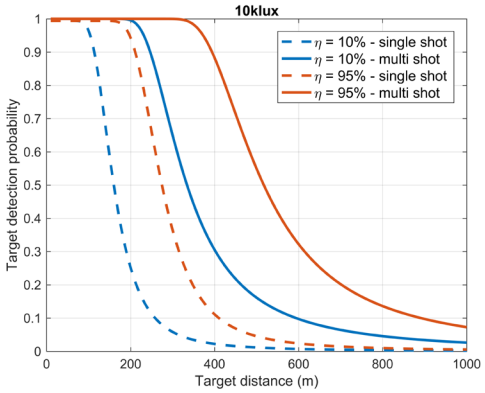

Figure 4. **Array performance at 10 klux** - The probability analysis shows ranging improvement when the system operates at a moderate ambient light level of 10 klux showing ranging over 200 m for low reflective targets.

number of unsuccessful measurement is obtained by $\mathcal{N}_{uns} = \mathcal{N}_{pulse}\,[1 - p_{success}(d)]$. The probability of the successful single-shot measurements to exceed the unsuccessful one is given by:

$$p_{multishot}(d) = \binom{\mathcal{N}_{pulse}}{\mathcal{N}_{uns}+1} \times p_{success}(d)^{\mathcal{N}_{uns}+1} \times \\ \times\,[1 - p_{success}(d)]^{\mathcal{N}_{pulse}-(\mathcal{N}_{unsucc}+1)} \quad (14)$$

We summarise the performance of the proposed SiPM array by showing the calculated probability of laser detection for the system described in Table I showing four different cases: a 10 % and a 95 % target both in single and multi-shot measurement approach, see Figure 3 and Figure 4 respectively for an ambient light level of 100 klux and 10 klux. We highlight a percentage of detection of 95% as a benchmark for confidence of the measurement and we show how the high detection efficiency of the SiPM combined with an appropriate dynamic range, i.e. number of SPAD cells per pixel, allow ranging of low reflective targets up to 115 m and beyond 150 m for high reflective objects in 100 klux. This is achieved by employing a multi-shot approach which sees the acquisition of 20 single-shots to generate a measurement. This shows an improvement from a maximum distance of 70 m and 90 m in a single shot approach respectively for a 10% and a 95% reflective target. This results demonstrate a significant improvement from state-of-the-art SiPM/SPAD based systems where the maximum achieved distance is in the order of 100 m for *white* targets (95% reflective) demonstrated in lower ambient light conditions (80 klux), [9]. We also predict longer ranging performance at 10 klux achieving over 230 m for low reflective objects and 370 m for bright targets, as shown in Figure 4.

IV. Conclusions

We have designed the first linear array sensor based on SiPM technology for long distance LiDAR systems based on horizontal scanning. The size of each SiPM pixel allows a sufficient dynamic range to be achieved thus avoiding saturation problems typical of SPAD-based systems without the need of additional filters. The ambient rejection is improved by the usage of bandpass filters around the chosen central wavelength without impacting the signal level. The high efficiency at 905 nm of the SiPMs allows the system to operate with an eye-safe laser transmitter at long distance even in full sunlight and light low reflective objects. The narrow angle of view of the sensor gives the system a high spatial resolution in both horizontal and vertical directions. The modelled results predict full operation in critical conditions such as 100 klux of sunlight incident on the target in the field of view of the sensor and a range of reflectivity from 5% to 95%. A probability of detection above 95% is predicted up to 100 m for dark objects. All is done achieving a full image of 800×16 covering $80°\times5°$ with a resolution of $0.1°\times0.312°$ with a 30 fps. The realized system is currently in testing at the time of this publication and experimental results are going to be compared to the predicted modeled performance.

References

[1] R. Agishev *et al.*, "Lidar with SiPM: Some capabilities and limitations in real environment," *Optics and Laser Technology*, vol. 49, pp. 86–90, 2013.

[2] G. Adamo *et al.*, "Time Of Flight measurements via two LiDAR systems with SiPM and APD," in *2016 AEIT International Annual Conference (AEIT)*, 2016, pp. 1–5.

[3] M. Perenzoni *et al.*, "A 64x64-Pixels Digital Silicon Photomultiplier Direct TOF Sensor With 100-MPhotons/s/pixel Background Rejection and Imaging/Altimeter Mode With 0.14 % Precision Up To 6 km for Spacecraft Navigation and Landing," *IEEE Journal of Solid-State Circuits*, vol. 52, no. 1, pp. 151–160, 2017.

[4] S. Dolinsky *et al.*, "Timing resolution performance comparison for fast and standard outputs of SensL SiPM," *IEEE Nuclear Science Symposium Conference Record*, 2013.

[5] A. Eisele *et al.*, "185 MHz Count Rate, 139 dB Dynamic Range Single-Photon Avalanche Diode with Active Quenching Circuit in 130nm CMOS Technology," *2011 International Images Sensor Workshop*, pp. 6–8, 2011.

[6] H. T. V. Dam *et al.*, "A Comprehensive Model of the Response of Silicon Photomultipliers," *IEEE Transactions on Nuclear Science*, vol. 57, no. 4, pp. 2254–2266, 2010.

[7] M. Grodzicka *et al.*, "Effective dead time of APD cells of SiPM," *IEEE Nuclear Science Symposium Conference Record*, pp. 553–562, 2012.

[8] ASTM, "Standard Tables for Reference Solar Spectral Irradiances : Direct Normal and," *Astm*, vol. 03, no. Reapproved, pp. 1–21, 2013.

[9] C. Niclass *et al.*, "A 100-m Range 10-Frame/s 340x96-Pixel Time-of-Flight Depth Sensor in 0.18μm CMOS," *IEEE Journal of Solid-State Circuits*, vol. 48, no. 2, pp. 559–572, 2013.